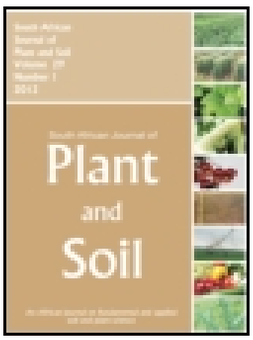

South African Journal of Plant and Soil

ISSN: 0257-1862 (Print) 2167-034X (Online) Journal homepage: http://www.tandfonline.com/loi/tjps20

Validation and downscaling of Advanced Scatterometer (ASCAT) soil moisture using ground measurements in the Western Cape, South Africa

Jason Moller, Nebo Jovanovic, Cesar L Garcia, Richard DH Bugan & Dominic Mazvimavi

To cite this article: Jason Moller, Nebo Jovanovic, Cesar L Garcia, Richard DH Bugan & Dominic Mazvimavi (2017): Validation and downscaling of Advanced Scatterometer (ASCAT) soil moisture using ground measurements in the Western Cape, South Africa, South African Journal of Plant and Soil, DOI: 10.1080/02571862.2017.1318962

To link to this article: http://dx.doi.org/10.1080/02571862.2017.1318962

Published online: 04 Sep 2017.

South African Journal of Plant and Soil 2017: 1–14
Printed in South Africa — All rights reserved

SOUTH AFRICAN JOURNAL OF
PLANT AND SOIL
ISSN 0257-1862 EISSN 2167-034X
http://dx.doi.org/10.1080/02571862.2017.1318962

Validation and downscaling of Advanced Scatterometer (ASCAT) soil moisture using ground measurements in the Western Cape, South Africa

Jason Moller[1], Nebo Jovanovic[1,2]*, Cesar L Garcia[3], Richard DH Bugan[2] and Dominic Mazvimavi[1]

[1] *Institute for Water Studies, University of the Western Cape, Bellville, South Africa*
[2] *CSIR, Natural Resources and Environment, Stellenbosch, South Africa*
[3] *Consejo Nacional de Investigaciones Cientificas y Tecnologicas (CONICET – UCC), Cordoba, Argentina*
** Corresponding author, email: njovanovic@csir.co.za*

Satellite-based remote sensing of soil water content (SWC) is a promising technology for hydrological applications to overcome large spatiotemporal variabilities of SWC. This study investigated the performance of the Advanced Scatterometer (ASCAT) soil moisture product on METOP satellite (~12.5 km and downscaled to ~1 km resolution), against ground measurements of SWC taken with a Hydrosense II probe along transects of 360–820 m on agricultural and natural land at locations in the Western Cape. The ASCAT products estimated fairly accurately seasonal trends of SWC; performance was better on lower slopes (R^2 = 0.66) and uniform vegetation. ASCAT 12.5 km performed better in estimating SWC than the downscaled product (average concordance coefficient = 0.60 and 0.39, and R^2 = 0.84 and 0.74, respectively). ASCAT 12.5 km was more responsive to rainfall events, whilst the downscaled product was more sensitive to vegetation characteristics (normalised difference vegetation index and land surface temperature). In situations with ground measurement networks and data availability constraints, remote sensing could be a feasible alternative to monitor SWC for hydrological applications at the meso-scale (regional scale).

Keywords: Malmesbury, NDVI, remote sensing, Riebeek, surface temperature

Introduction

Accurate quantification of components of the water cycle, especially precipitation, evapotranspiration (ET) and soil moisture, is important in the management of water resources, especially in arid and semi-arid regions (Bugan et al. 2012). Ground-based measurements are generally resource-consuming at large catchment scales. Attempts were made in the past to model water variables such as rainfall using historic time series (Valipour 2016) and soil moisture (Sinclair and Pegram 2010), whilst ET estimates are generally based on weather data (Allen et al. 1998). Numerous empirical and physical methods to estimate reference ET were tested in different climatic conditions (Valipour 2012, 2014a, 2014b; Valipour et al. 2017). However, it is only with the advancement of remote sensing technologies that the coverage of water-cycle components at scales appropriate for water resources management and high frequency is possible (Bastiaanssen et al. 1998a, 1998b; Su 2002; Nadler et al. 2005; Allen et al. 2007a, 2007b; Glenn et al. 2007; Mu et al. 2007).

Amongst the water-cycle components, soil water content (SWC) exerts considerable influence on hydrological and pedogenic processes (Martinez et al. 2008) and is variable in time and space near the surface. The temporal and spatial dynamics of SWC are influenced by topography, soil properties, vegetation cover, depth to the water table and meteorological conditions (Gómez-Plaza et al. 2001). Soil water content is also a key variable in understanding land–atmosphere interactions, as the transfer of water from the soil to the atmosphere via ET influences wet and dry anomalies over continental regions (Bosch et al. 2006). As a result, SWC is a dominant factor in shaping an ecosystem's response to the physical environment (Wei 1995), and influences growth of rangeland plants and cultivated crops, and the susceptibility of soils to degradation processes (Tansey et al. 1999) and flooding (Brocca et al. 2010; Koster et al. 2010; Brocca et al. 2011). For these reasons, soil moisture has been recently listed as one of the 'essential climate variables' for describing the Earth's climate (GEO 2014).

Approaches for estimating SWC include ground-based measurements, estimations based on remote sensing, and modelling (Martinez et al. 2008). The direct measurement of SWC is in many cases not feasible due to the high degree of spatiotemporal variability of soil characteristics of an area, combined with the relatively small volumes investigated (Lacava et al. 2010), which is only a few square metres or less (Brocca et al. 2007; Penna et al. 2009). This has resulted in a lack of SWC ground-monitoring networks. Remote sensing offers a feasible alternative to ground measurements of SWC, and provides estimates averaged over large areas, and is potentially more cost effective and efficient than collecting ground data (Jovanovic et al. 2014).

Amongst the remote sensing methods for the estimation of SWC, microwave techniques are promising because they offer daily coverage and are capable of providing estimates in all weather conditions. Albergal et al. (2009) argued

that the L-band (frequency of 1–2 GHz) is the optimal microwave wavelength for sensors to detect changes in SWC in the top layer of the soil. There are currently several satellite sensors operating at or near this frequency, such as the Soil Moisture and Ocean Salinity (SMOS), the Advanced Microwave Scanning Radiometer for the Earth Observing System (AMSR-E) on board the Aqua satellite, and the Advanced Scatterometer (ASCAT) on board the Meteorological Operational (METOP) satellite. ASCAT, which operates in the C-band at a frequency just above the L-band (5.255 GHz) offers the best combination of spatial (~12.5 km) and temporal (1–2 d) resolution. This product was found to perform well compared with ground measurements in several validation studies (Albergal et al. 2009; Brocca et al. 2011). However, there have not been studies comparing ASCAT SWC estimates with ground measurements in semi-arid areas of South Africa.

Remote sensing products for soil moisture estimation with reasonably short revisit times are generally characterised by coarse spatial resolution (>10 km^2) (Brocca et al. 2011). This spatial resolution may be too coarse for certain water management applications at the meso-scale level (Schultz 1994), and therefore there is a need to investigate downscaling of satellite soil moisture estimates to finer resolution. Downscaling of SWC can broadly be grouped into stochastic and deterministic approaches. One of the major shortcomings of stochastic approaches is that the downscaled products are often not derived from physically based inputs and therefore can have several possible solutions (Kim and Barros 2002; Boucher 2007). Deterministic approaches, on the other hand, use estimates of land surface attributes for downscaling and thus rely on data that have physical meaning. Methods for SWC downscaling include the use of fractal interpolation with fine-scale surface information (Kim and Barros 2002), interpolation of passive microwave data with fine-scale active microwave data (Bindlish and Barros 2002; Das et al. 2011), distributed hydrological modelling with local information on topography (Pellenq et al. 2003), brightness temperature linear regression (Chauhan et al. 2003), downscaling using soil evaporative efficiency (Merlin et al. 2008) and multifractal modelling (Mascaro et al. 2011).

Studies have established that spatial variations of radiant surface temperature strongly depend on surface SWC (Merlin et al. 2006), assuming that the higher the soil water content, the higher the soil evaporation and the lower the soil temperature. Vegetation also plays an important role in this relationship, as there is no universal relationship between soil moisture and land surface temperature (Chauhan et al. 2003). Unique relationships between soil moisture availability and land surface temperature relative to the corresponding normalised difference vegetation index (NDVI) over specific climatic conditions and land surface types have been established (Carlson et al. 1994; Chauhan et al. 2003). Accurate soil moisture estimation from optic/infrared (IR) remote sensing techniques is affected by vegetation cover, soil texture, organic matter and surface roughness that introduce noise and thus complicate the interpretation of sensor measurements (Asner 1998; Ben-Dor et al. 1999). A method was proposed by Chauhan et al. (2003) to overcome these limitations by combining coarse-resolution microwave soil moisture retrievals with finer resolution optic/IR remote sensing parameters. This was achieved through determining relationships between surface soil moisture and surface temperature for specific vegetation types and densities, which in conjunction with the coarse-resolution microwave soil moisture estimates (~12.5 km) were used to obtain soil moisture at a higher spatial resolution (~1 km).

This review of the international body of knowledge identified that validation of spatiotemporal dynamics of SWC against ground data was not sufficiently addressed for application of SWC estimates in semi-arid regions, especially in southern Africa. In addition, to improve water management a downscaling method for coarse-spatial-resolution satellite SWC estimates should be investigated. The objective of this study was therefore to validate ASCAT estimates of SWC against ground measurements taken along transects in a semi-arid region of the Western Cape province, South Africa. We used both coarse-resolution (~12.5 km) satellite SWC estimates and values downscaled to ~1 km resolution using the brightness temperature linear regression model of Chauhan et al. (2003). The goal was to explore a critical variable for water management, closely linked to ET, in the southern part of Africa where water is a constraint for development.

Methods

Study site description

Two study areas in the semi-arid western coastal region of the Western Cape province were selected to investigate the feasibility of using satellite information to estimate SWC (Figure 1). One site was in the vicinity of Malmesbury and the other in the Riebeek Valley with different soil characteristics and hydrological properties. The topography of the area is gently undulated. The climate is Mediterranean with warm dry summers and wet cool winters. Mean daily temperatures vary from about 7 °C in July to about 27.9 °C in February. Most of the rainfall occurs between April and October, and the average annual rainfall is 450 mm y^{-1}. Rainfall events occur over a few days with significant periods of clear weather in between and are a result of cyclonic and frontal activity. The mean annual A-pan evaporation rate is estimated to be around 2 150 mm y^{-1} and the daily rate exceeds rainfall for approximately 70% of the time. Daily rainfall and temperatures were measured at Malmesbury and Riebeek at stations WS1 and WS2 (Figure 1).

Malmesbury is situated in the Groen River catchment. This area is characterised by deep well-leached, generally acidic and coarse sandy soils of marine and aeolian origin. The land cover is dominated by cultivated lands and natural vegetation. Farming activities include wheat cultivation mixed with pastures and vineyards. The natural vegetation is dominated by Atlantis Sand Plain Fynbos, most of which is about 1–1.5 m tall emergent shrubs with a dense mid-story of other shrubs and a ground layer of recumbent shrubs, herbaceous species, geophytes and grasses with occasional succulents (Rebelo et al. 2006). The Riebeek Valley is situated in the Berg River catchment. Relatively shallow, brownish sandy loam soils are developed on Malmesbury shales, which are prone to cracking after heavy rains. The topsoil varies in thickness between

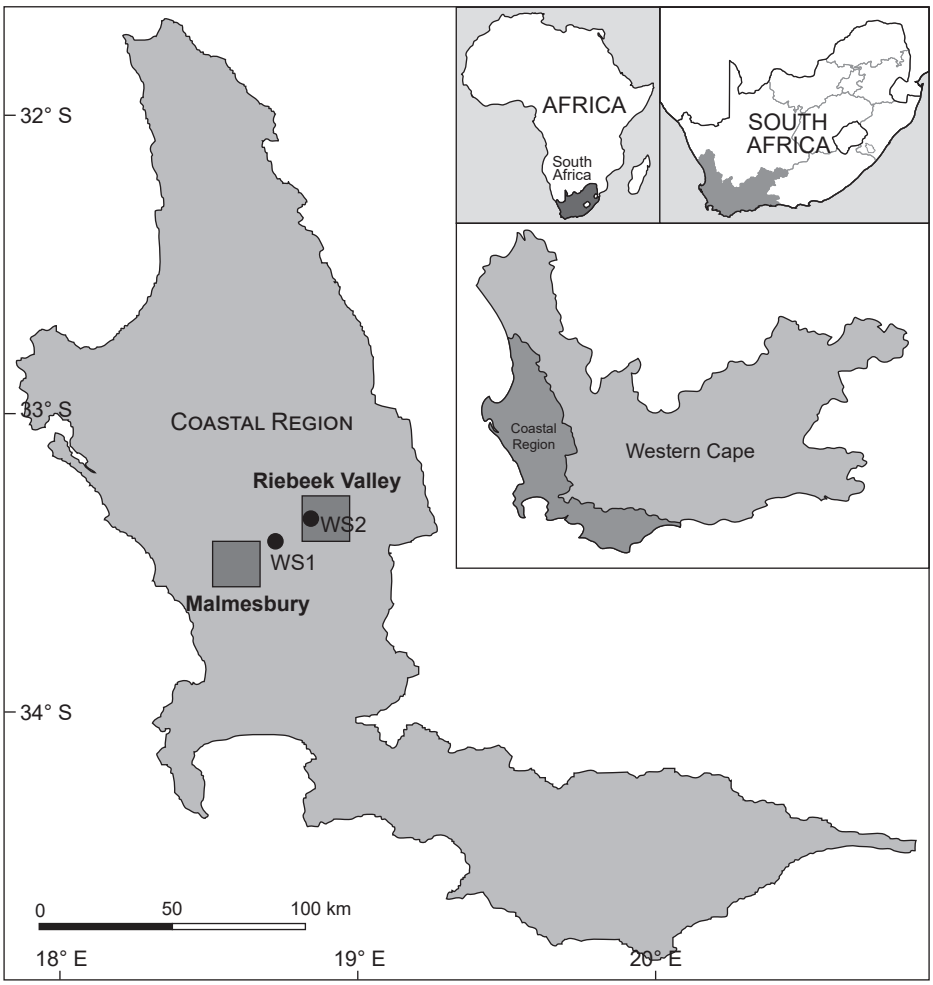

Figure 1: Study site locations at Malmesbury and Riebeek Valley within the coastal region of the Western Cape province of South Africa. Rainfall stations WS1 (South African Weather Services; 33.4720° S, 18.7180° E) and WS2 (Agricultural Research Council; 33.35115° S, 18.83849° E) are shown. The squares correspond to the 12.5 km pixels of ASCAT

0.5 and 1 m and is red and yellow in colour. The land cover is dominated by cultivated lands and pastures with very little natural vegetation. The two sites were deemed sufficiently different from each other, but still representative of the general environmental conditions of the region. Analysis of SWC estimated from remote sensing data was done for two 12.5 km ASCAT pixels with each pixel covering the selected study sites (Figure 1).

Sampling transects

Ground measurements of SWC were taken along hillslope transects in order to capture as much as possible of any spatial variability in soil moisture. Sampling transects were chosen to represent a range of elevations, slopes, land use/land cover (LU/LC) conditions and soil types within the two 12.5 km ASCAT pixels. A digital elevation model, produced by the Shuttle Radar Topography Mission (SRTM) with a spatial resolution of 30 m (SRTM30), was obtained from the National Aeronautics and Space Administration (NASA) (NASA 2013). Land cover information was generated by digitising the various land-cover classes in the open source GIS software package ILWIS (Schouwenburg 2013), using cadastral maps of the area obtained from the National Survey General of South Africa (produced in May 2012). Cadastral maps were used for this purpose as they represented the most accurate LU/LC information available in these areas. Digital elevations models and land-cover maps of the two 12.5 km ASCAT pixels are shown in Figure 2. The total area covered by each of the defined land-cover classes are presented in Table 1. Both study areas have similar proportion of the area with wheat/pasture. The Malmesbury site had a higher proportion with natural vegetation and a lower percentage of vineyard and urban areas than the Riebeek Valley site.

Based on elevation, land cover, soil types and accessibility to sites/farms, six sampling transects were selected along hillslopes characterised by different land covers (Figure 2, bottom panel). The transects varied in length from 360 to 820 m, and had slopes ranging from 1.7% to 6.3% (Table 2). A detailed description of the transects can be found in Moller (2014).

There were no appreciable visually discernible differences in soil texture and colour along each transect. Soil analyses were therefore done for each transect on three composite

topsoil samples taken in the upslope and downslope areas, and are summarised in Table 3. Soil textural analyses were done using the settling or sedimentation method, which then allowed for the identification of soil class based on the USDA soil textural classification system (Soil Survey Division Staff 1993). The bulk densities were also determined for three soil samples taken with Kopecki cylinders and averaged. The Malmesbury transects had mostly sandy soils with the exception of the upslope areas at Rondevlei and Nieuwepost farms (Table 2), which are loamier due to the relatively high amounts of silt. The Riebeek transects had predominantly loamy sand and sandy loam, with higher silt and clay amounts than Malmesbury transects.

Ground measurements of soil water content

Due to the relatively large number of SWC measurements required to characterise spatiotemporal variabilities along transects, a portable Hydrosense II soil moisture probe (Campbell Scientific Inc., Logan, UT, USA) was used to record volumetric SWC. This instrument works on the principle of time domain reflectometry and it makes use of a CS659 soil water sensor. Measurements of SWC were made at monthly intervals from 19 July 2013 until 27 January 2014, which covered the wet and dry seasons. Sampling points were at 20–25 m intervals along the transects, which enabled the variability in SWC along the hillslopes to be determined. Three replicated measurements were taken

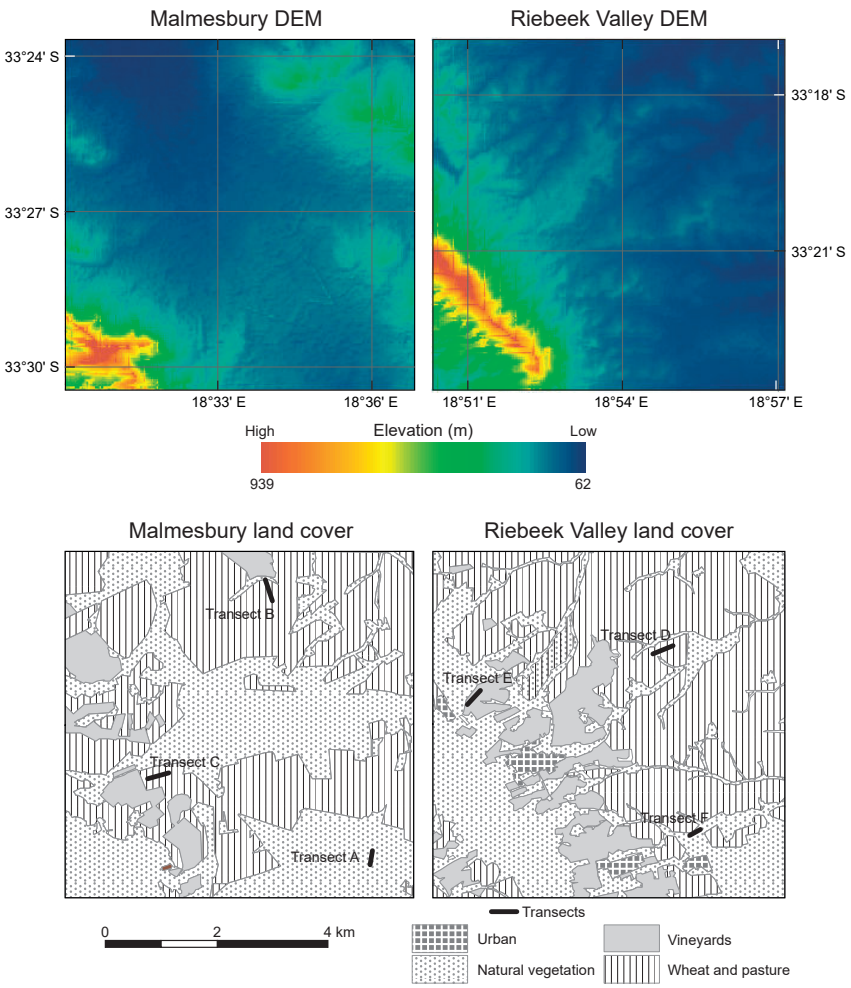

Figure 2: Digital elevation models (DEMs) for the Malmesbury and Riebeek Valley study sites, corresponding to the ASCAT 12.5 km pixels, obtained from NASA's SRTM30 (NASA 2013) (top panel). Land-cover maps of the Malmesbury and Riebeek Valley study sites, obtained from the National Survey General (produced in May 2012), depicting the dominant land-cover types as well as the six sampling transects (bottom panel)

Table 1: Land cover as a percentage of the total area for the Malmesbury and Riebeek Valley ASCAT pixels

Site	Land-cover type (%)			
	Wheat/pasture	Vineyard	Natural vegetation	Urban
Malmesbury	48.78	7.32	43.9	0
Riebeek	48.78	13.82	35.77	1.63

at each sampling point at 0–10 cm soil depth (length of the CS659 rods is 12 cm). Measurements were taken at the exact same georeferenced points during each sampling campaign. The calibration of the Hydrosense II probe was adjusted for the soil type of the transects using SWC determined through gravimetric sampling (Moller 2014).

Satellite-derived estimations of soil water content

ASCAT has been operating on the METOP satellite since 2006 and is a C-band scatterometer (5.255 GHZ, VV polarised) with a radiometric accuracy better than ~0.3 dB (Verspeek et al. 2010). C-band scatterometers are used for soil moisture retrieval with the Vienna University of Technology (TUWIEN) change detection algorithm proposed by Wagner et al. (1999) and improved by Naeimi et al. (2009). Soil moisture retrieved using ASCAT has a ~12.5 km spatial resolution.

ASCAT is a real-aperture radar instrument, which measures radar backscatter on either side of the METOP satellite track, and generates two 550 km wide swaths of data (Albergal et al. 2009). A triplet of backscattering coefficients ($\sigma°$) is produced by ASCAT using three separate antenna beams on both sides of METOP, by averaging several radar signals made at 45°, 90° and 135° azimuth angles relative to the satellite track. The set of backscattering coefficients at different azimuth angles allows for the determination of the yearly cycle of the backscatter incident relationship, which is essential for correcting seasonal vegetation effects (Gelsthorpe et al. 2000; Bartalis et al. 2007). The backscattering coefficients extrapolated to a reference angle at 40° [$\sigma°(40)$] are scaled using the lowest and highest values of $\sigma°(40)$ over an extended period of time to determine wet and dry limiting cases (Wagner et al. 1999). ASCAT-derived soil moisture content (θ_A) is therefore given as:

$$\theta_A(t) = \frac{\sigma^o(40,t) - \sigma^o{}_{dry}(40,t))}{\sigma^o{}_{wet} - \sigma^o{}_{dry}(40,t)} \quad (1)$$

where limiting cases are denoted by $\sigma°_{dry}(40, t)$ for backscatter at the dry limit and $\sigma°_{wet}(40, t)$ for backscatter at the wet limit, and t is time. This equation is representative of the top few centimetres of soil and can be applied if the ground is not frozen (Schmugge 1983). Soil moisture is given as the degree of saturation in percentages from 0% (dry) to 100% (saturated). In our case, the dry and saturated values were normalised for the absolute minimum and maximum readings obtained with the Hydrosense II probe at each transect. ASCAT overpass and measurement times are twice per day, in the morning and early evening. Jackson (1980) recommended using morning soil moisture estimates in order to avoid the daytime decoupling

Table 2: Characteristics of transects selected for ground measurements of soil moisture

Site	Transect	Location	Main land cover	Coordinates and altitude (m)	Length (m)	Change in elevation (m)	Slope (%)
Malmesbury	A	Riverlands	Natural vegetation	33.4892° S, 18.6110° E; 140 m 33.4926° S, 18.6107° E; 130 m	380	10	3.80
	B	Rondevlei	Agricultural	33.4077° S, 18.5763° E; 192 m 33.4053° S, 18.5700° E; 151 m	650	41	6.31
	C	Nieuwepost	Agricultural	33.4689° S, 18.5264° E; 120 m 33.4678° S, 18.5345° E; 108 m	780	12	1.54
Riebeek	D	Goedetrou	Agricultural	33.3155° S, 18.9156° E; 106 m 33.3110° S, 18.9219° E; 84 m	820	22	2.68
	E	De Gif	Agricultural	33.3261° S, 18.8551° E; 231 m 33.3308° S, 18.8527° E; 207 m	560	24	4.29
	F	De la Gift	Natural vegetation	33.3725° S, 18.9259° E; 93 m 33.3736° S, 18.9228° E; 87 m	360	6	1.67

Table 3: Results of soil analyses for samples collected along the transects used for ground measurements of soil moisture

Transect	Particle size (%)			Soil texture	Bulk density (g cm^{-3})
	Silt	Clay	Sand		
A upslope	2.94	2.35	94.71	Sandy	1.38
A downslope	3.71	3.71	92.59	Sandy	1.46
B upslope	6.54	4.62	88.84	Loamy sand	1.52
B downslope	3.84	4.42	91.75	Sandy	1.52
C upslope	6.07	5.69	88.25	Loamy sand	1.92
C downslope	3.47	5.01	91.53	Sandy	1.98
D upslope	22.99	10.55	66.46	Sandy loam	1.45
D downslope	32.10	18.59	49.31	Loam	1.58
E upslope	22.42	17.60	59.99	Sandy loam	1.56
E downslope	12.14	6.70	81.16	Loamy sand	1.66
F upslope	21.35	3.42	75.24	Loamy sand	1.46
F downslope	51.26	0.00	48.74	Silty loam	1.50

effect between the top few centimetres of soil and the layer beneath it.

Downscaling coarse-resolution soil moisture estimates (~12.5 km) to a finer spatial resolution (~1 km) was done using the method proposed by Chauhan et al. (2003). Land surface temperature and near-surface soil moisture are spatially related because evaporation from the soil surface keeps the land surface temperature low (Merlin et al. 2006). The NDVI was used to empirically calibrate the correlation between land surface temperature and soil moisture content for various vegetation covers. These relationships are referred to as the 'universal triangle'. The regression relationships between land surface temperature, NDVI and SWC can be determined from Equations 2 to 4:

$$T^* = \frac{T - T_0}{T_S - T_0} \tag{2}$$

$$\mathrm{NDVI}^* = \frac{\mathrm{NDVI} - \mathrm{NDVI}_0}{\mathrm{NDVI}_S - \mathrm{NDVI}_0} \tag{3}$$

where T is land surface temperature (°C), the subscripts S and 0 stand for maximum and minimum values, and the superscript * indicates prime (dimensionless). Carlson et al. (1994) expressed the relationship between SWC, NDVI* and T^* through a regression formula:

$$\mathrm{SWC}(t) = \sum_{i=0}^{i=n} \sum_{j=0}^{j=n} a_{ij} \mathrm{NDVI}^{*(i)} T^{*(j)} \tag{4}$$

where i and j indicate the order of the polynomial. Equation 4 can be written in the form of a second-order polynomial:

$$\mathrm{SWC}(t) = \alpha_{00} + \alpha_{10}\mathrm{NDVI}^* + \alpha_{20}\mathrm{NDVI}^{*2} + \alpha_{01}T^* + \alpha_{02}T^{*2} + \alpha_{11}\mathrm{NDVI}^*T^* + \alpha_{21}\mathrm{NDVI}^{*2}T^* + \alpha_{12}\mathrm{NDVI}^*T^{*2} + \alpha_{22}\mathrm{NDVI}^{*2}T^{*2} \tag{5}$$

Third-order terms are negligible and they can be ignored (Chauhan et al. 2003). For the calibration of the coefficients α_{00} to α_{22}, coarse-resolution soil moisture ($\mathrm{SWC_c}$) is substituted into the left-hand side of Equation 5, while the corresponding T^* and NDVI* values for the same resolution are substituted on the right-hand side. Once the coefficients are determined, fine resolution T^* and NDVI* values are substituted on the right-hand side of the equation, which enables estimation of SWC at fine resolution ($\mathrm{SWC_F}$).

This approach can be employed only on cloudless days as this uses optic/IR data. The assumption is that these regression relationships are constant over the entire microwave soil-moisture pixel, which may not be valid especially in areas with high surface and meteorological heterogeneity. For this reason, one of the criteria for selection of pixels and transects was the homogeneity of the agricultural areas, so as to minimise effects of surface and microclimatic heterogeneity within the coarse-resolution satellite soil-moisture pixels. The data sets of T and NDVI used for the downscaling algorithm at ~1 km resolution were acquired from NASA (MODIS satellite) through their data dissemination portal (US Geological Survey 2014).

Data processing and statistical analyses

To understand how transects are related to each other and to the ASCAT pixels, a principal component analysis (PCA) was performed using all transect characteristics. The first two components were graphed using a bi-plot (Gabriel 1971) to facilitate interpretation of results.

Validation of satellite estimates of SWC (both coarse-resolution and downscaled fine-resolution ASCAT estimates) was done by comparison with ground measurements obtained with the Hydrosense II probe. Spatiotemporal trends of ground measurements of SWC and ASCAT-derived SWC were analysed using Pearson's correlation coefficient and concordance analysis (Lin 1989, 2000). While the Pearson's coefficient (Pcc) measures the agreement in the temporal behaviour between observed and estimated pairs, the concordance coefficient (Ccc) provides the degree to which pairs deviate from a 1:1 behaviour (a 45° line through the origin in a graph) and thus evaluates both the precision and the accuracy of different methods over the same sample. Normally, to test if the Pearson correlation between estimated and observed data is statistically significant, a linear regression is used. Due to the small sample size, linear regression assumptions were not met; instead a simple linear mixed model that accounts for autocorrelation was used to determine the p value (limiting significance at $P < 0.05$).

Results and discussion

Spatiotemporal variations in ground measurements of soil water content

A PCA was performed to summarise the transect characteristics regarding the soil properties and location attributes (Figure 3). The first two components explained 72% of the total variability. The first component clearly differentiated transects from the two sites, showing a high correlation of the Malmesbury site with the sand content of the soil and the strong silt imprint of the Riebeek site. The second component sorted transects in relation to their length, soil

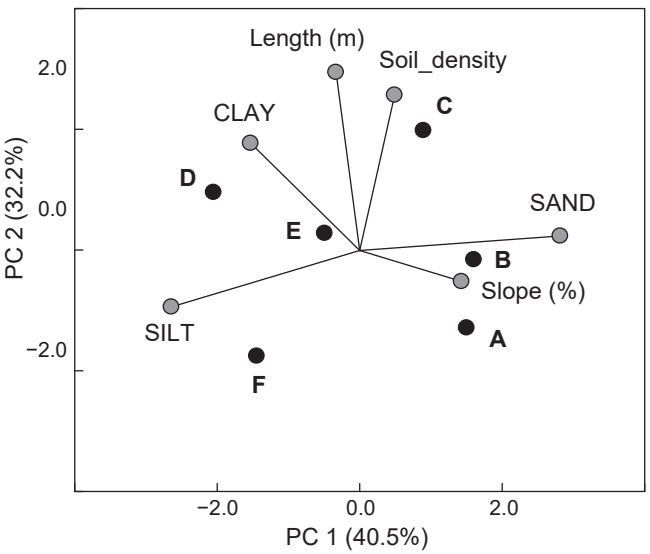

Figure 3: Principal component analysis summarising the transect characteristics (soil properties and location attributes)

density and clay soil content. Overall, the analysis showed that both sites could be differentiated by soil properties and that transects were evenly distributed within the two sites to cover a similar range of internal variability (from the ASCAT 12.5 km perspective).

The SWC measured using the Hydrosense II probe increased during the wet season from July to September 2013, and then decreased during the dry season (Figure 4). The example in Figure 4 is for transect D, which was characterised by average slope and bulk density, and a fair distribution of particle sizes compared with the other transects (Tables 2 and 3). The SWC was fairly uniform along transect D on all sampling days (Figure 4), with a similar response observed in transects C and E. The SWC showed large variation along transects A, B and F, and with a tendency for SWC to increase towards the downslope part, due to the presence of shallow groundwater. Figure 4 also shows a peak in SWC in the middle

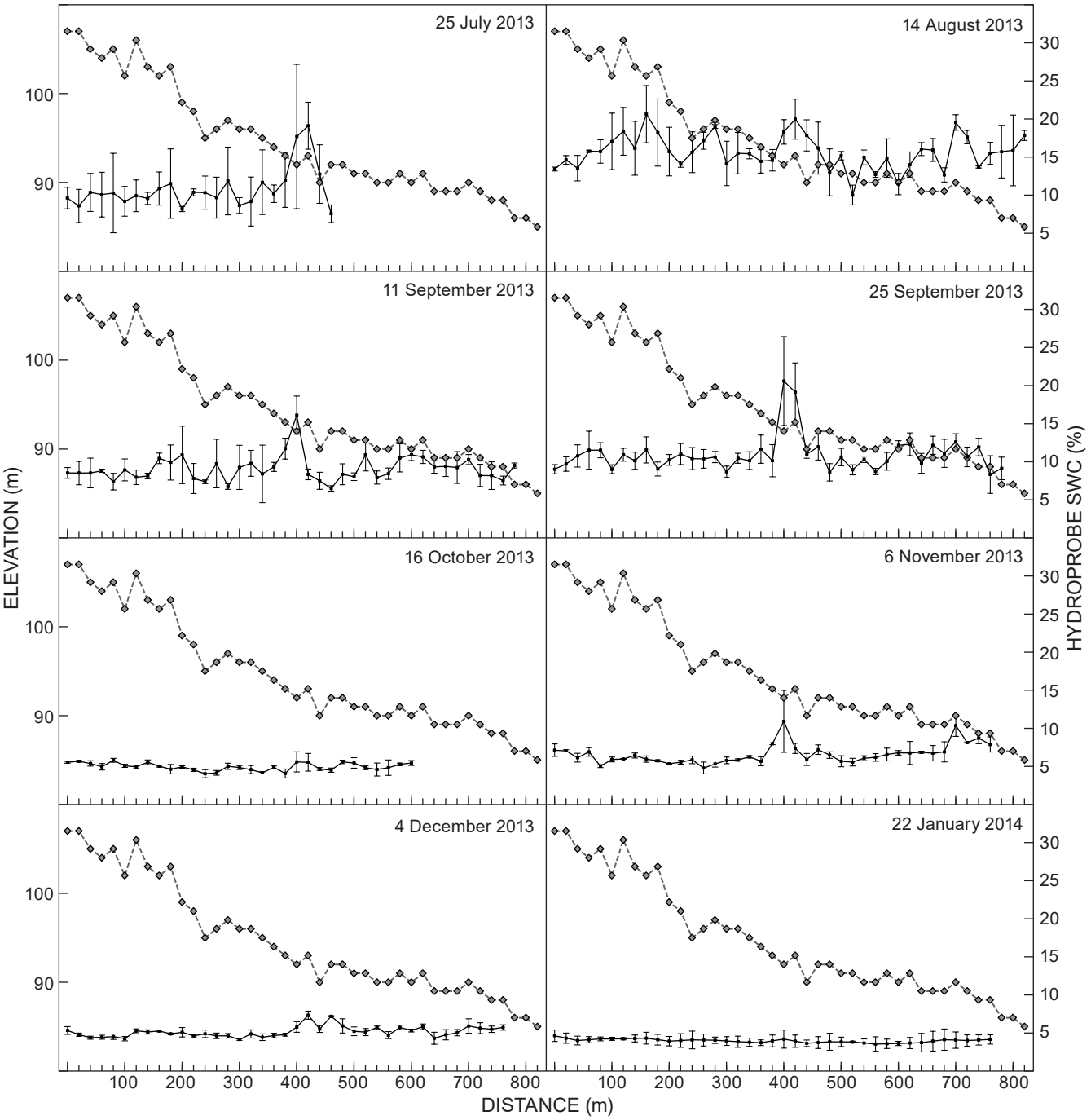

Figure 4: Volumetric soil water content (SWC) measured with a Hydrosense II probe along Transect D from 25 July 2013 to 22 January 2014 (solid line). The ground elevation is also shown (dashed line). The error bars indicate the standard deviation of three measurements of SWC at each sampling point

of the transect during winter; this is due to an elevation anomaly represented by a man-made anti-erosion contour. This land management feature retards overland flow and causes water to pond on its upslope side. The variability of SWC at each sampling point (Figure 4) was large during the rainy season and low during the dry season. Transect D is in agricultural land and during the wet winter water redistributes in the soil unevenly due to land management and forms ponds on the soil surface. Soils were completely dry in January 2014 with little variability along the hillslopes and between sampling points. The SWC values were generally high along the sandier Malmesbury transects during the wet periods, but low during the dry periods in comparison with the Riebeek site with generally loamy soils. Transects A and F, which had natural vegetation, had higher SWC during the wet periods compared with agricultural land in their respective pixels.

Downscaling ASCAT 12.5 km to a 1 km SWC product

In order to calibrate the coefficients α_{00} to α_{22} in the downscaling calculation (Equation 5), all NDVI pixel values were plotted against *T* values for the entire study period to produce the universal triangle. A triangle was produced for each 12.5 km ASCAT pixel at each study site (Figure 5). From these triangles, the maximum and minimum NDVI and *T* values needed in the downscaling algorithm were determined. The universal triangles for Malmesbury and Riebeek (Figure 5) were very similar with regards to maximum and minimum values for *T* and NDVI as depicted by the dashed lines on the top, bottom and left sides of Figure 5. The top left corners of the triangles represent wet conditions where *T* is low and NDVI values are high as experienced during late July until early September. The bottom right-hand corner of the triangles is indicative of pixel values that are dry with high *T* and low NDVI. Three groups

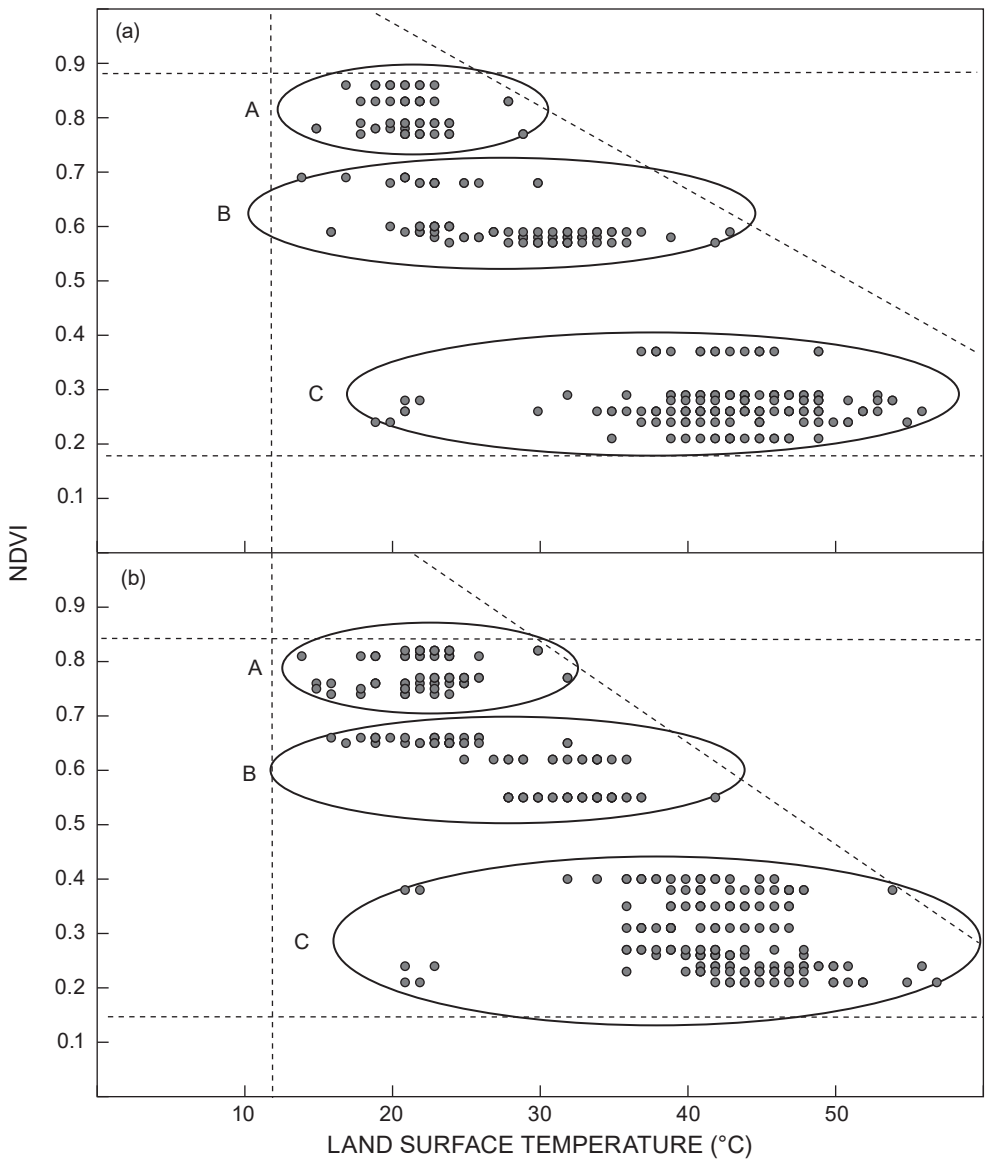

Figure 5: Universal triangle depicting the normalised difference vegetation index (NDVI) and land surface temperature (°C) at Malmesbury (top) and Riebeek Valley (bottom)

of values are formed generally representing wet, drying and dry conditions as outlined by A, B and C (Figure 5). Some extreme values exceeding 50 °C were recorded. The MODIS *T* product is reported to give surface temperature values within 1 °C accuracy (Wang and Liang 2009).

Maximum and minimum *T* and NDVI values were then used to determine their scaled values using Equations 2 and 3. Scaled *T** and NDVI* values were then used in Equation 5, and coefficients α_{00} to α_{22} were calibrated by inserting ASCAT SWC in the left-hand side of the equation. The calibration was done using the least two squares method. Calibrated coefficients were obtained for each pixel, as each pixel had a unique relationship between *T*–NDVI and SWC. The calibrated coefficients are summarised in Table 4.

Testing 12.5 km ASCAT and downscaled 1 km SWC at transect scale

The comparison of ASCAT SWC (12.5 km), downscaled SWC (1 km) and average ground measurements of SWC is presented in Figure 6 for each transect on days when ground measurements were taken. During the wet period (July–September 2013), the 12.5 km ASCAT SWC estimates varied between 11.3% and 29.2% for the Malmesbury site, and between 6.6% and 26.7% at the Riebeek site. This was followed by a drying period (October–November 2013), which stabilised around December, when values were generally <5% at all transects. The 12.5 km ASCAT SWC estimates at both sites showed high sensitivity to rainfall, resulting in high peaks of soil moisture corresponding to rainfall events on

Table 4: Calibrated coefficients for the brightness temperature linear regression model for the Malmesbury and Riebeek Valley study sites

Site	α_{00}	α_{01}	α_{10}	α_{11}	α_{02}	α_{20}	α_{12}	α_{21}	α_{22}
Riebeek Valley	4.76	−3.8	4.75	16.09	−2.04	5.19	−4.43	4.17	−1.14
Malmesbury	9.91	−8.94	12.69	17.21	−3.91	2.33	−2.47	4.05	−2.28

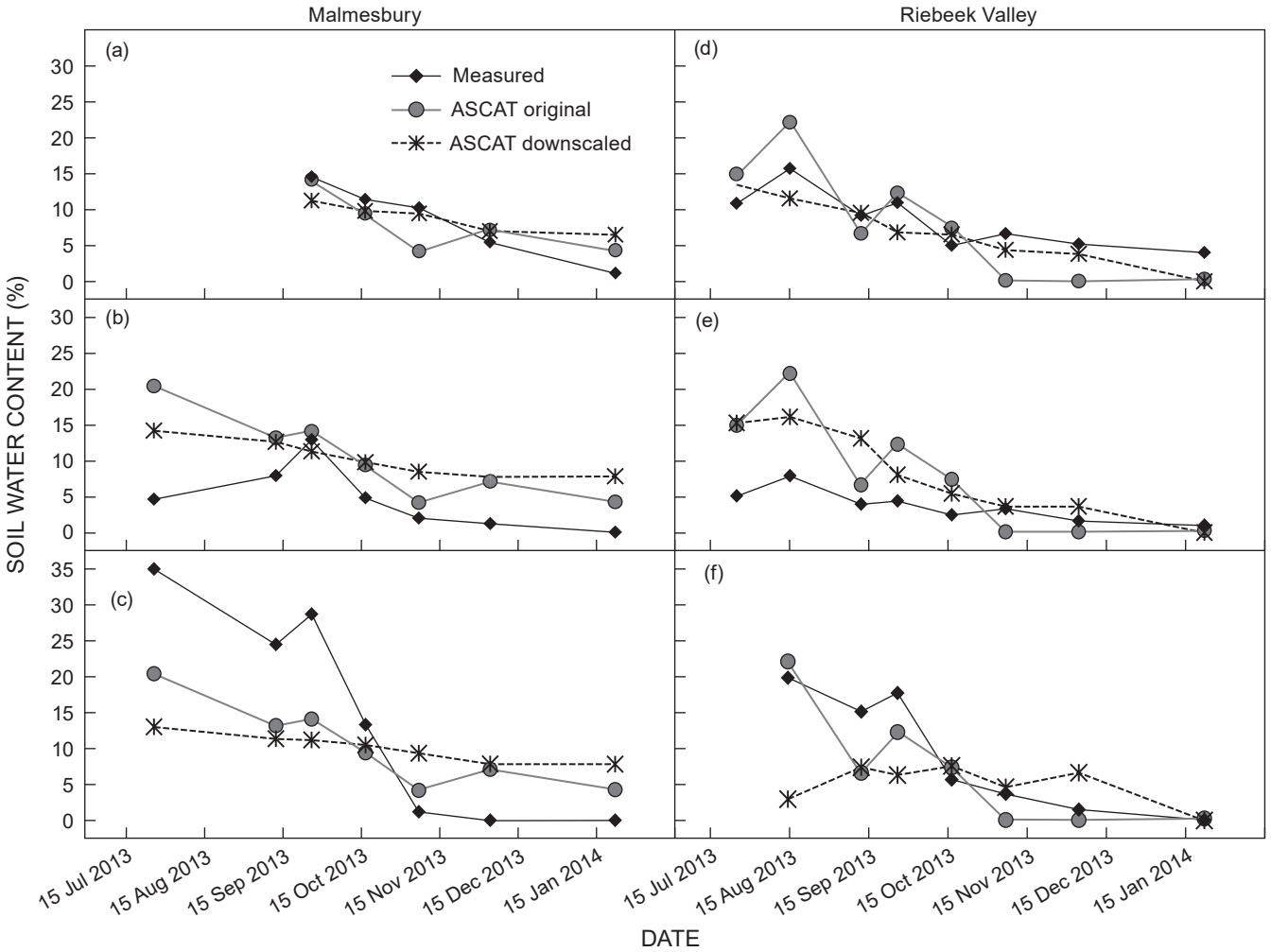

Figure 6: Measured soil water content (SWC), ASCAT 12.5 km SWC and downscaled 1 km SWC for transects at Malmesbury (a–c) and Riebeek Valley (d–f)

31 October 2013, 16 November 2013 and 8 January 2014 (Figure 7).

All downscaled SWC estimates decreased from the wet winter to the dry summer. A comparison with rainfall data (Figure 7), however, showed that downscaled SWC values were less responsive to rainfall compared with 12.5 km ASCAT SWC. This means that, in general, the ASCAT SWC estimates were more aligned to the measured SWC time series (Figure 6), whilst the downscaled SWC responded to temperature and NDVI, and to a lesser extent to individual rainfall events.

Two tests based on a pair comparison (Pcc and Ccc) were performed to determine which remotely sensed SWC provided a better representation of the SWC measured in the transects (Table 5). The Pcc is a more commonly used index that evaluates the linear relationships for the two methods, and shows how two data sets co-vary but cannot detect systematic bias (Krause et al. 2005). In that regard, the Ccc offered a more robust way to evaluate the accuracy of the ASCAT (12.5 km and downscaled) estimation of SWC. For example, transect C showed high Pcc correlations (Pearson) for both products, but the Ccc showed a better performance of the original ASCAT to estimate SWC (see also Figure 6c for the sub- and supra-bias). The combined analysis with the two methods helped to identify the best performance product for each transect. For all other transects except transect A, the SWC estimated by the 12.5 km ASCAT was closer to the field-measured values than those estimated using the downscaling algorithm. In addition, it can be noted that transects with the worst performance in estimating SWC were B and E. These two transects are the ones that exhibit the greatest slope. In general, the higher correlation coefficients between 12.5 km ASCAT SWC and measured SWC (Figure 8) related to transects with smaller slopes. This clearly indicates that the accuracy of satellite estimations of SWC (according to two indicators) decreases with increasing slope.

Chauhan et al. (2003) suggested that there are two possible sources of error attributed to the brightness temperature linear regression model: (1) regression errors based on the coarse-resolution SWC estimates and transferred to downscaled estimates via the regression coefficients α_{ij} and (2) precision errors attributed to inaccuracies of *T* and NDVI values. Regression errors for these two study sites, in terms of coarse-resolution SWC inputs for calibration of α_{ij}, were within acceptable accuracy

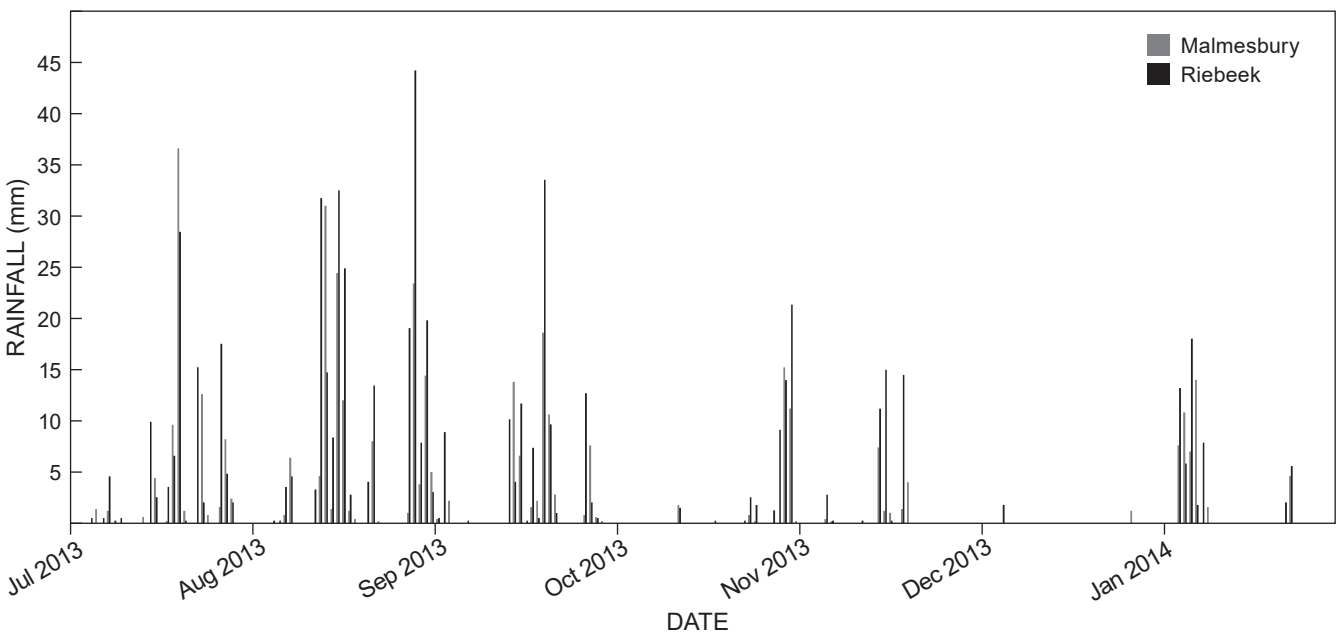

Figure 7: Daily rainfall at Malmesbury and Riebeek during the study period (July 2013 to January 2014)

Table 5: Performance comparison of the 12.5 km ASCAT and downscaled 1 km soil water content (SWC) estimates

SWC product	Transect					
	A	B	C	D	E	F
Pearson correlation coefficient (Pcc)						
ASCAT 12.5 km	0.74	0.60	0.96*	0.92*	0.92*	0.88*
ASCAT 1 km	0.98*	0.61	0.95*	0.80*	0.88*	0.22
Concordance coefficient (Ccc)						
ASCAT 12.5 km	0.71	0.37	0.62	0.73	0.37	0.85
ASCAT 1 km	0.64	0.24	0.22	0.75	0.38	0.11

* $p < 0.05$

ranges as these estimates were found to represent average moisture conditions reasonably well at both sites for the duration of the study. There were, however, some concerns about the accuracy of the ASCAT product during the dry period, but based on the method of calibration (least difference of two squares method), low values were likely to have small effects on the calibration of the regression coefficients.

Precision errors of the *T* and NDVI products (at 1 km scale) were assumed to have a small effect, as the accuracy of these products was well validated and also scaled values were used to reduce possible errors. It was, however, noted that some *T* values were extremely high at both study areas during the summer period (>50 °C). The issue of precision error does arise with regard to homogeneity or heterogeneity of land cover, as well as local topography along the various transects and their immediate surrounding areas covering the 1 km pixel. The lower the vegetation cover and the slope, the higher the expected accuracy of *T* and NDVI at high resolution (Walker et al. 2003). In our case, the downscaled 1 km SWC method performed best on the transect with moderate vegetation cover in a flat area (transect A) and on the transect with uniform grassland on a moderate slope (transect D, Ccc in Table 5). Chauhan et al. (2003) proposed the use of albedo to strengthen the relationship between *T*–NDVI and SWC. This, however, may not account for fine-scale land surface heterogeneities. The downscaled method was also less responsive to rainfall than the coarse-resolution ASCAT (Figure 6). There were slight variations in daily *T* values that may have been influenced by rainfall events, but NDVI showed no daily response to rainfall and thus downscaled 1 km SWC showed less daily variations compared with 12.5 km ASCAT SWC.

In each 12.5 km ASCAT pixel, there were three transects measured with the Hydrosense II probe and three downscaled pixels coinciding with each transect (Figures 1 and 2). The values of the field-measured SWC for the three transects were averaged and compared with the 12.5 km ASCAT pixel SWC value. This comparison (Figure 9, Table 6) showed that the 12.5 km ASCAT is generally a better estimator of SWC than the downscaled product. Moreover, it is interesting to note in Figure 9 that downscaled estimates of SWC present a constant downward trend, something noticeable also in Figure 6, and do not reflect the peaks during the rainy season (Figure 7). This is a clear indication that a dominant variable in the algorithm producing the downscaled product is the vegetation (captured by NDVI). This raises a concern about the downscaling technique for SWC estimation, as the estimation seems to be dependent on land cover/phenology changes, represented by land use, and affected by factors such as fires, vegetation greenness and root depths.

Conclusions

In this study, the estimation of SWC using remote sensing data was investigated as an alternative to time- and resource-consuming ground measurements in the semi-arid regions of the Western Cape province of South Africa. The results of the comparison of ASCAT SWC estimates and ground measurements demonstrated that the coarse-resolution (12.5 km) ASCAT does estimate soil moisture with an acceptable accuracy level and is capable of detecting changes in SWC caused by rainfall

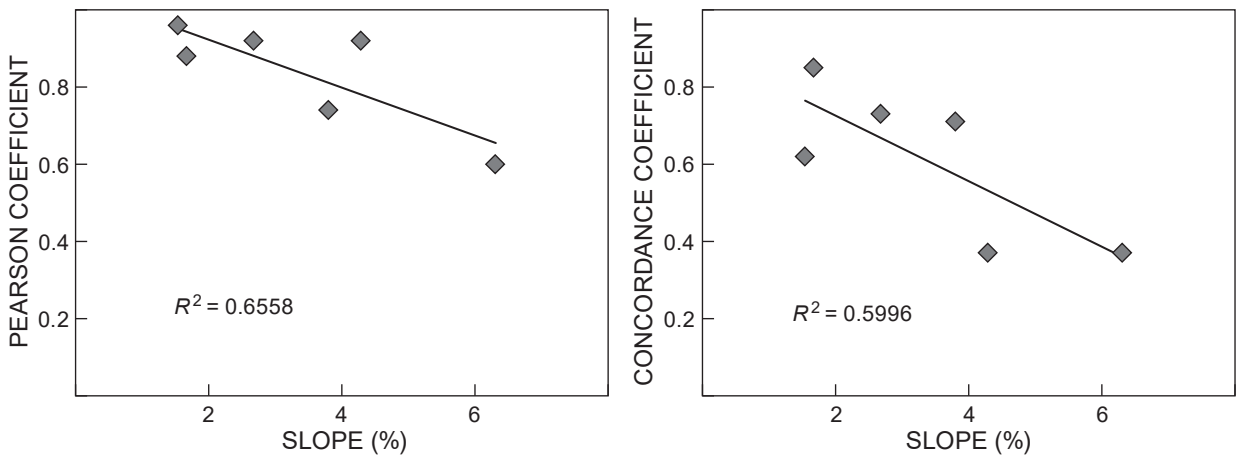

Figure 8: Performance coefficients of the 12.5 km ASCAT vs measured soil water contents as a function of the transect slope

Table 6: Performance comparison of averaged 12.5 km ASCAT and averaged downscaled 1 km soil water content (SWC) estimates

SWC product	Pearson correlation coefficient (Pcc)		Concordance coefficient (Ccc)	
	Malmesbury	Riebeek Valley	Malmesbury	Riebeek Valley
ASCAT 12.5 km	0.93*	0.89*	0.89	0.74
ASCAT 1 km average	0.96*	0.66	0.51	0.66

* $p < 0.05$

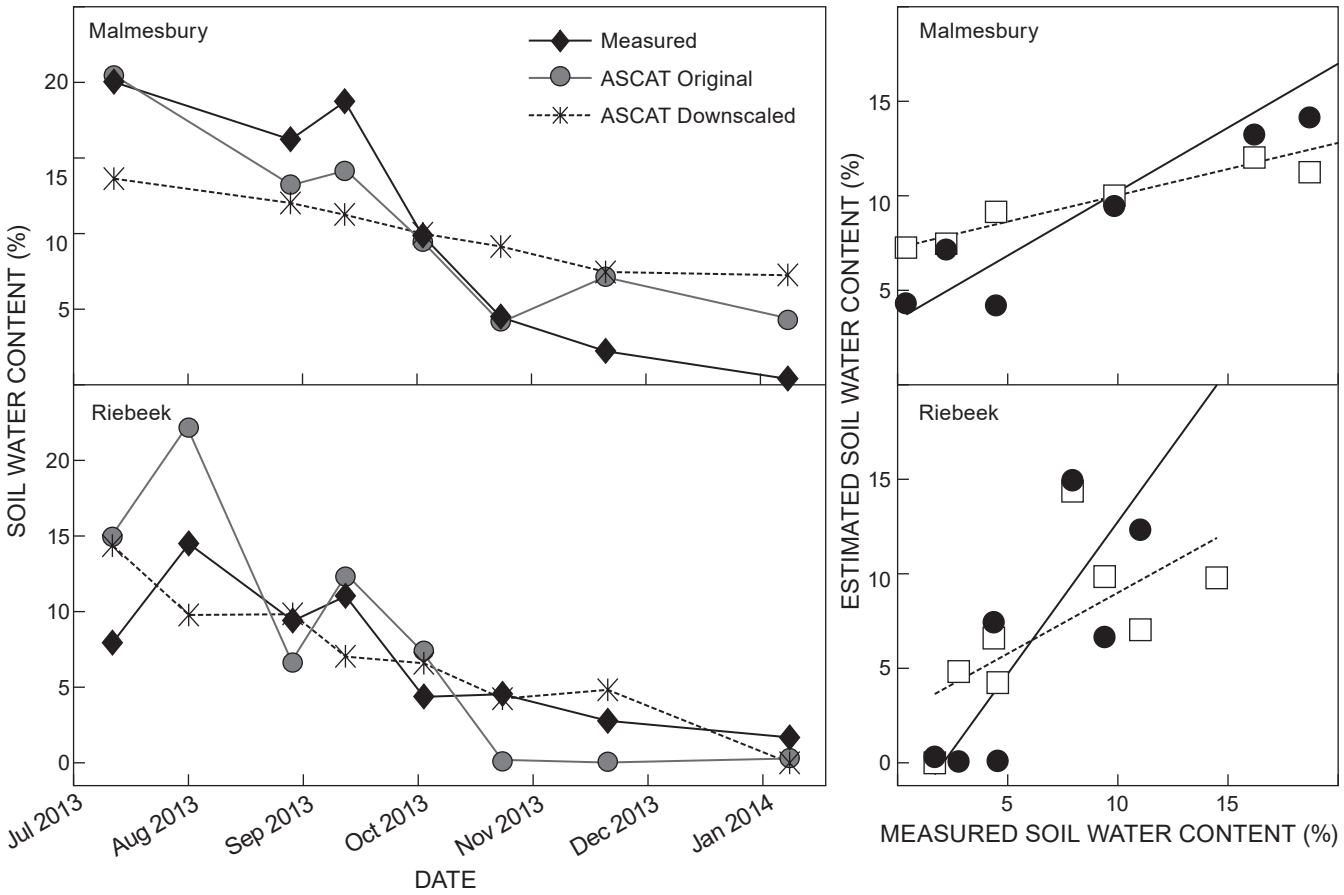

Figure 9: Comparison of the time series (measured, 12.5 km ASCAT and downscaled 1 km soil water content SWC) for Malmesbury and Riebeek (left graphs). Measured vs estimated SWC pairwise view (right graphs)

events. The accuracy of SWC derived from ASCAT is, however, low during dry periods, possibly as a result of increased topographic effects on backscatter sensitivity and reduced microwave penetration of the soil surface in drier conditions. Satellite-derived SWC performance was associated with slope, and it was the most accurate in areas with low to moderate slopes and uniform vegetation. Nevertheless, additional studies with more sampling units are recommended to test the effect of the slope on satellite-derived SWC estimation. The main sources of error were linked to the fine-scale surface heterogeneities, such as non-uniform vegetation, slopes or man-made features. Differences between satellite-derived SWC estimates and ground measurements were also partly due to the comparison of different depths of SWC measured by the soil moisture probe and estimated remotely. Downscaling of soil moisture estimates to 1 km resolution also provided reasonable results when examining general seasonal SWC variability, but the performance was generally poorer than the 12.5 km ASCAT product due to the dependency of the downscaling method on vegetation characteristics (NDVI and land surface temperature). Further research needs to be conducted to improve understanding of spatial aggregation effects of land surface parameters and to develop more accurate methods for downscaling coarse-resolution SWC satellite data.

Due to the lack of ground measurement networks and data availability constraints, remote sensing may be a feasible approach to monitor SWC for hydrological applications at the meso-scale (regional scale). The performance of ASCAT in this study suggests that in the semi-arid regions of southern Africa this product can be a useful alternative to other data sources. Nevertheless, land slope should be considered and further studies are recommended in other types of climate and regions. Application of ASCAT can also aid in obtaining information on the spatiotemporal variability of soil moisture. It is also possible to calibrate the satellite-derived SWC against specific points on the ground. However, where high-precision estimates are needed, such as applications in agricultural irrigation, remote sensing data may not be adequate. *In situ* SWC monitoring still provides crucial information needed to better understand remote sensing-derived records and for downscaling remotely sensed data.

Acknowledgements — The authors acknowledge the CSIR Parliamentary Grant for funding the research. Riverlands Nature Reserve (CapeNature), the Swartland Municipality and the farmers that made their land available for conducting the research are also acknowledged, as well as the South African Weather Services and the Agricultural Research Council for providing rainfall data. We also thank the anonymous reviewers that helped improve the quality and clarity of this publication.

References

Albergal C, Rüdiger C, Carre D, Calvet JC, Fritz N, Naeimi V, Bartalis Z, Hasenauer S. 2009. An evaluation of ASCAT surface moisture products with in-situ observations in southwestern France. *Hydrology and Earth System Sciences* 13**:** 115–124.

Allen RG, Pereira LS, Raes D, Smith M. 1998. *Crop evapotranspiration: guidelines for computing crop water requirements. Irrigation and Drainage Paper* 56. Rome: Food and Agriculture Organization of the United Nations.

Allen RG, Tasumi M, Morse A, Trezza R, Wright JL, Bastiaanssen W, Kramber W, Lorite I, Robinson CW. 2007b. Satellite-based energy balance for mapping evapotranspiration with internalized calibration (METRIC)—applications. *Journal of Irrigation and Drainage Engineering* 133: 395–406.

Allen RG, Tasumi M, Trezza R. 2007a. Satellite-based energy balance for mapping evapotranspiration with internalized calibration (METRIC)—model. *Journal of Irrigation and Drainage Engineering* 133: 380–394.

Asner GP. 1998. Biophysical and biochemical sources of variability in canopy reflectance. *Remote Sensing of Environment* 64: 134–153.

Bartalis Z, Wagner W, Naeimi V, Hasenauer S, Scipal K, Bonekamp H, Figa J, Anderson C. 2007. Initial soil moisture retrievals from the METOP-A Advanced Scatterometer (ASCAT). *Geophysical Research Letters* 34: L20401.

Bastiaanssen WGM, Menenti M, Feddes RA, Holtslag AAM. 1998a. A remote sensing surface energy balance algorithm for land (SEBAL) 1. Formulation. *Journal of Hydrology* 212–213: 198–212.

Bastiaanssen WGM, Pelgrum H, Wang J, Ma Y, Moreno JF, Roebink GJ, van der Wal T. 1998b. A remote sensing surface energy balance algorithm for land (SEBAL) 2. Validation. *Journal of Hydrology* 212–213: 213–229.

Ben-Dor E, Irons JR, Epema GF. 1999. Soil reflectance. In: Rencz AN (ed.), *Remote sensing for earth science: manual of remote sensing*. New York: John Wiley and Sons. pp 111–188.

Bindlish R, Barros AP. 2002. Sub-pixel variability of remotely sensed soil moisture: an inter-comparison study of SAR and ESTAR. *IEEE Transactions on Geoscience and Remote Sensing* 40: 326–337.

Bosch DD, Lakshmi V, Jackson TJ, Choi M, Jacobs JM. 2006. Large scale measurements of soil moisture for validation of remotely sensed data: Georgia soil moisture experiment of 2003. *Journal of Hydrology* 323: 120–137.

Boucher A. 2007. Downscaling of satellite remote sensing data: application to land cover mapping. PhD thesis, Standford University, USA.

Brocca L, Hasenauer S, Lacava T, Melone F, Moramarco T, Wagner W, Dorigo W, Matgen P, Martínez-Fernández J, Llorens P, Latron J, Martin C, Bitelli M. 2011. Soil moisture estimation though ASCAT and AMSR-E sensors: an intercomparison and validation study across Europe. *Remote Sensing of Environment* 115: 3390–3408.

Brocca L, Melone F, Moramarco T, Morbidelli R. 2010. Spatial-temporal variability of soil moisture and its estimation across scales. *Water Resources Research* 46**:** W02516.

Brocca L, Morbidelli R, Melone F, Moramarco T. 2007. Soil moisture spatial variability in experimental areas of central Italy. *Journal of Hydrology* 333: 356–373.

Bugan RDH, Jovanovic NZ, de Clercq WP. 2012. The water balance of a seasonal stream in the semi-arid Western Cape (South Africa). *Water SA* 38: 201–212.

Carlson T, Gillies R, Perry E. 1994. A method to make use of thermal infrared temperature and NDVI measurements to infer surface soil water content and fractional vegetation cover. *Remote Sensing Reviews* 9: 161–173.

Chauhan NS, Miller S, Ardanuy P. 2003. Spaceborne soil moisture estimation at high resolution: a microwave-optical/IR synergistic approach. *International Journal of Remote Sensing* 24: 4599–4622.

Das NN, Entekhabi D, Njoku EG. 2011. An algorithm for merging SMAP radiometeer and radar data for high resolution soil moisture retrieval. *IEEE Transactions on Geoscience and Remote Sensing* 49: 1504–1512.

Gabriel KR. 1971. The biplot graphic display of matrices with application to principal component analysis. *Biometrika* 58: 453–467.

Gelsthorpe RV, Schied E, Wilson JJW. 2000. ASCAT-Metop's Advanced Scatterometer. *European Space Agency Bulletin* 102: 19–27.

GEO (Group on Earth Observations). 2014. *The GEOSS water strategy: from observations to decisions*. Tokyo: Japan Aerospace Exploration Agency.

Glenn EP, Huete A, Nagler P, Hirschboeck KK, Brown P. 2007. Integrating remote sensing and ground methods to estimate evapotranspiration. *Critical Reviews in Plant Science* 26: 139–168.

Gómez-Plaza A, Martínez-Mena M, Albaladejo J, Castillo VM. 2001. Factors regulating spatial distribution of soil water content in small catchments. *Journal of Hydrology* 253: 211–226.

Jackson TJ. 1980. Profile soil moisture from space measurements. *Journal of the Irrigation and Drainage Division* 106: 81–92.

Jovanovic N, Garcia CL, Bugan RDH, Teich I, Garcia Rodriguez CM. 2014. Validation of remotely-sensed evapotranspiration and NDWI using ground measurements at Riverlands, South Africa. *Water SA* 40: 211–220.

Kim G, Barros AP. 2002. Downscaling of remotely sensed soil moisture with a modified fractal interpolation method using contraction mapping and ancillary data. *Remote Sensing of Environment* 83: 400–413.

Koster RD, Mahanama SPP, Livneh B, Lettenamaier DP, Reichle RH. 2010. Skill in streamflow forecasts derived from large-scale estimates of soil moisture and snow. *Nature Geoscience* 3: 613–616.

Krause P, Boyle DP, Bäse F. 2005. Comparison of different efficiency criteria for hydrological model assessment. *Advances in Geosciences* 31: 89–97.

Lacava T, Brocca L, Calice G, Melone F, Moramarco T, Pergola N, Tramutoli V. 2010. Soil moisture variations monitoring by AMSU-based soil wetness indices: a long-term inter-comparison with ground measurements. *Remote Sensing of Environment* 114: 2317–2325.

Lin LIK. 1989. A concordance correlation coefficient to evaluate reproducibility. *Biometrics* 45: 255–268.

Lin LIK. 2000. Correction: a note on the concordance correlation coefficient. *Biometrics* 56: 324–325.

Martinez C, Hancock GR, Kalma JD, Wells T. 2008. Spatio-temporal distribution of near-surface and root zone soil moisture at the catchment scale. *Hydrological Processes* 22: 2699–2714.

Mascaro G, Vivoni ER, Deidda R. 2011. Soil moisture downscaling across climate regions and its emergent properties. *Journal of Geophysical Research: Atmospheres* 116: D22114.

Merlin O, Chehbouni A, Kerr YH, Goodrich DC. 2006. A down-scaling method for distributing surface soil moisture within a microwave pixel: application to the Monsoon '90 data. *Remote Sensing of Environment* 101: 379–389.

Merlin O, Walker JP, Chehbouni A, Kerr Y. 2008. Towards deterministic downscaling of SMOS soil moisture using MODIS derived soil evaporative efficiency. *Remote Sensing of Environment* 112: 3935–3946.

Moller J. 2014. The use of remote sensing for soil moisture estimation using downscaling and soil water balance modelling in Malmesbury and the Riebeek Valley. MSc thesis, University of

the Western Cape, South Africa.
Mu Q, Heinsch FS, Zhao M, Running SW. 2007. Development of a global evapotranspiration algorithm based on MODIS and global meteorology data. *Remote Sensing of Environment* 111: 519–536.
Nadler P, Cleverly J, Lampkin D, Glenn E, Huete A. 2005. Predicting riparian evapotranspiration from MODIS vegetation indices and meteorological data. *Remote Sensing of Environment* 94: 17–30.
Naeimi V, Scipal K, Bartalis Z, Hasenauer S, Wagner W. 2009. An improved soil moisture retrieval algorithm for ERS and METOP scatterometer observation. *IEEE Transactions on Geoscience and Remote Sensing* 47: 1999–2013.
NASA (National Aeronautics and Space Administration). 2013. SRTM 90m Digital Elevation Data from the CHIAR Consortium for Spatial Information. Available at http://gcmd.nasa.gov/records/GCMD_CGIAR_SRTM_90.html [accessed November 2013].
Pellenq J, Kalma J, Boulet G, Saulnier GM, Woodridge S, Kerr Y, Chehbouni A. 2003. A disaggregation scheme for soil moisture based on topography and soil depth. *Journal of Hydrology* 276: 112–127.
Penna D, Borga M, Norbiato D, Dalla Fontana G. 2009. Hillslope scale soil moisture variability in a steep alpine terrain. *Journal of Hydrology* 364: 311–327.
Rebelo AG, Boucher C, Helme N, Mucina L, Rutherford MC, Smit WJ, Powrie LW, Ellis F, Lambrechts JJ, Scott L et al. 2006. Fynbos biome. In: Mucina L, Rutherford MC (eds), *The vegetation of South Africa, Lesotho and Swaziland. Strelitzia* 19. Pretoria: South African National Biodiversity Institute.
Schmugge TJ. 1983. Remote sensing of soil moisture: recent advances. *IEEE Transactions on Geoscience and Remote Sensing* 21: 336–344.
Schowenburg ML. 2013. ILWIS 3.8 Map Visualization Based on ILWIS 3.8.3. Twente: ITC, University of Twente.
Schultz GA. 1994. Meso-scale modelling of runoff and water balances using remote sensing and other GIS data. *Hydrological Sciences Journal* 39: 121–142.
Sinclair S, Pegram GGS. 2010. A comparison of ASCAT and modelled soil moisture over South Africa, using TOPKAPI in land surface mode. *Hydrology and Earth System Sciences* 14: 613–626.
Soil Survey Division Staff. 1993. S*oil survey manual. US Department of Agriculture Handbook* no. 18. Washington, DC: Soil Conservation Service, US Department of Agriculture.
Su Z. 2002. The Surface Energy Balance System (SEBS) for estimation of turbulent heat fluxes. *Hydrology and Earth System Sciences* 6: 85–99.
Tansey KJ, Millington AC, Battikhi AM, White KH. 1999. Monitoring soil moisture dynamics using satellite imaging radar in northeastern Jordan. *Applied Geography* 19: 325–344.
US Geological Survey. 2014. Land Processes Distributed Active Archive Center. Available at https://lpdaac.usgs.gov/data [accessed January 2014].
Valipour M. 2012. Ability of Box-Jenkins models to estimate of reference potential evapotranspiration (a case study: Mehrabad Synoptic Station, Tehran, Iran). *IOSR Journal of Agriculture and Veterinary Science* 1(5): 1–11.
Valipour M. 2014a. Analysis of potential evapotranspiration using limited weather data. *Applied Water Science* 7: 187–197.
Valipour M. 2014b. Application of new mass transfer formulae for computation of evapotranspiration. *Journal of Applied Water Engineering and Research* 2: 33–46.
Valipour M. 2016. How much meteorological information is necessary to achieve reliable accuracy for rainfall estimations? *Agriculture* 6(4): 53.
Valipour M, Gholami Sefidkouhi MA, Raeini−Sarjaz M. 2017. Selecting the best model to estimate potential evapotranspiration with respect to climate change and magnitudes of extreme events. *Agricultural Water Management* 180: 50–60.
Verspeek J, Stoffelen A, Portabella M, Bonekamp H, Anderson C, Saldana JF. 2010. Validation and Calibration of ASCAT using CMOD5.n. *IEEE Transactions on Geoscience and Remote Sensing* 48: 386–395.
Wagner W, Lemoine G, Rott H. 1999. A method for estimating soil moisture from ERS scatterometer and soil data. *Remote Sensing of Environment* 70: 191–207.
Walker JP, Houser PR, Willgoose GR. 2003. Active microwave remote sensing for soil moisture measurement: a filed evaluation using ERS-2. *Hydrological Processes* 17**:** 1975–1997.
Wang KS, Liang S. 2009. Evaluation of ASTER and MODIS land surface temperature and emissivity products using surface longwave radiation observations at SURFRAD sites. *Remote Sensing of Environment* 113: 1156–1165.
Wei MY (ed.). 1995. *Soil moisture: report of a workshop held in Tiburon, California, 25–27 January 1994. NASA Conference Publication* 3319. Washington, DC: NASA Headquarters.

Received 9 December 2016, revised 7 April 2017, accepted 7 April 2017
Associate Editor: Sunette Laurie